LASER INTERFEROMETER GRAVITATIONAL WAVE OBSERVATORY

LIGO Laboratory / LIGO Scientific Collaboration

LIGO-T1000276-v5 January 25, 2013

Output Mode Cleaner Design

Koji Arai, Sam Barnum, Peter Fritschel, Jeff Lewis, Sam Waldman

This is an internal working note
of the LIGO Laboratory

California Institute of Technology
Massachusetts Institute of Technology
LIGO Hanford Observatory
LIGO Livingston Observatory

http://www.ligo.caltech.edu/

1 Introduction

The Advanced LIGO Output Mode Cleaner (OMC) enables the DC readout sensing scheme of the interferometer's differential arm length (DARM). The OMC is a short (~1 m long) Fabry-Perot cavity, used to filter out the fundamental DC carrier mode and its audio frequency phase sidebands from the RF fields and higher order spatial modes. Functionally, the OMC is positioned between the anti-symmetric output of the interferometer and the DC readout photodiodes (DCPDs) used for sensing DARM. Physically, the OMC is located in the output vacuum chamber (HAM6), mounted in a double suspension that sits on the HAM-ISI single-stage active isolation platform. The OMC *assembly* includes both the OMC and the DCPDs.

2 Design Overview

The OMC is designed as a rigid optical cavity, constructed in a 4-mirror bow-tie configuration in order to reduce retro-reflection from the cavity. The cavity mirrors are bonded to a glass breadboard; the photodiodes used for the DC readout of the interferometer are also mounted to this breadboard to ensure that the beam pointing onto the DCPDs is extremely stable. Two quadrant photodiodes (QPDs) are also mounted on the glass breadboard, and a small fraction of the light incident on the OMC is directed to these QPDs to monitor and aid in the alignment of the incident beam to the cavity.

Two of the OMC cavity mirrors are mounted on PZTs for actuation and control of the cavity length. The OMC is locked to the interferometer beam with a dither scheme (modulation of the cavity length, demodulation of the transmitted light, feedback applied to the cavity length).

The OMC transmitted light is split 50-50 between two photodiodes. The use of two photodiodes provides the ability to characterize correlated and uncorrelated noises, allows higher OMC transmitted power (if necessary), and provides redundancy.

The OMC assembly—consisting of the glass breadboard, the cavity, and the DCPDs and QPDs—is mounted in a double-stage suspension for vibration isolation. The actively damped suspension also provides DC/slow control of the position of the OMC assembly. The preamplifiers for the DCPDs are mounted at the top of the suspension structure, so that they are in close proximity to the diodes. The preamps for the QPDs are mounted outside the vacuum chamber.

3 Cavity optical design

The choice of cavity finesse is a trade-off between filtering of unwanted fields (high finesse) and transmission efficiency for the desired TEM_{00} mode (low finesse). We set a minimum transmission efficiency of 98%, assuming total round trip loss of 140 ppm (10 ppm scatter loss per mirror, plus 50 ppm transmission for the high-reflectors). The relation between resonant transmission, loss, and finesse is: $T_{FP} \approx 1 - L_{rt}F/\pi$, where L_{rt} is the round trip loss and F is the finesse. Then the condition $T_{FP} \geq 0.98$ implies $F \leq 450$. To have a little more tolerance to loss, we have chosen a **finesse of 400**.

The other optical parameters that must be chosen together are the cavity and cavity g-factor. In general, these parameters should be determined such that the filtering performance of the cavity is maximized. The resulting cavity parameters are listed in Table 1.

Cavity round trip length	1.132 m
Free spectral range	264.8 MHz
ROC of high-reflectors	Spec: 2.5m; Meas: 2.575 m
g-parameter	0.7717 (hor.); 0.7729 (vert.)
Higher order mode spacing	57.95 MHz (h); 58.10 MHz (v)
Angle of incidence on cavity mirrors	4 degrees
Polarization	p-pol/horizontal
Input/output coupler transmission	Spec: 8300ppm; Meas: 7930ppm
High-reflector transmission	Spec: 50ppm; Meas: 46-51ppm
Finesse	390
Beam sizes ($1/e^2$ radius)	
In/out couplers	0.50 mm
Curved (HR) mirrors	0.57 mm
DC PDs	0.52 mm
QPDs (radius/Gouy phase)	0.41 mm/4.1 deg 0.60 mm/35 deg

Table 1. Parameters of the OMC cavity design.

The radius-of-curvature (RoC) of the OMC curved mirrors is specified to be 2.5 m. This number was decided based on the calculation of frequency spacing between undesirable modes and the main carrier resonance. This calculation is described in detail in the technical note T1000276. The actual curvatures of the delivered mirrors were characterized with the transverse mode spacing of a FP cavity formed by the OMC curved and flat mirrors. The average RoC of the 6 mirrors was measured to be 2.575 ± 0.005 m after removing a couple of outliers.

For the further optimization of the cavity length, a power-law model of the higher-order mode (HOM) content at the dark port was used. The model was derived from measurements on the eLIGO interferometers, where the OMCs were scanned to measure the HOM content. The details of the HOM model are found in G1201111. In addition there is TEM_{00} mode power from the RF

sidebands, primarily the 45 MHz sidebands. All of these field components are included in a calculation of the power transmitted by the OMC cavity, as a function of the cavity g-parameter.

For the measured curved mirror RoC, a minimum in the transmission of HOMs and RF SBs occurs at a cavity length of 1.132 ± 0.005 m. At this point, the transmission of the undesirable modes is expected to be 10^{-5} W/W, relative to the power incident on the interferometer. Therefore only 1mW of the undesirable modes is expected for an incident power of 100W. Details of the calculation are presented in G120111.

The non-zero angle of incidence (θ_{AOI} = 4 deg) of the beams on the curved mirrors causes a small astigmatism of the cavity modes. The ratio between the effective curvatures of the mirror for the horizontal and vertical modes is $\cos^2\theta_{AOI} = 0.995$. The transverse mode spacing for the horizontal and vertical modes are different by 6×10^{-4} in units of free-spectral-range (FSR). As this is smaller than the cavity line width of 2.5×10^{-3} FSR, the higher-order modes are overlapped. Thus the effect of the astigmatism appears as broadening of the higher-order mode resonances.

It should be noted that an alternative to the bowtie cavity geometry was considered as a candidate. This is called the "No-BS" configuration in T1000276, as the cavity has two output couplers, each having half the transmission of the input coupler. We actually coated some curved mirrors to have the "half" transmission, and confirmed that any degradation of the cavity transmission due to mirror transmission mismatch would be negligible. No significant disadvantage was found except that the No-BS configuration has a slightly longer optimum cavity length (1.175m) compared to the bowtie cavity. As we did not find any serious issue with the use of the beamsplitter for the DC photodetectors in the eLIGO OMC, we adopted the bowtie configuration.

4 Scattered light

4.1 Back-scattering

The OMC will be the largest source of light scattered back into the interferometer (retro-reflected). This is one of the main reasons it is isolated with a double-suspension. The retro-reflection comes from the resonant build-up of a counter-propagating mode in the OMC, sourced by backscattering of the main circulating field from the cavity mirrors. For scattering from a single cavity mirror, the fractional power scattered into the backward propagating mode is $BRDF(\theta)\cdot(\lambda^2/\pi\omega^2)$, where *BRDF* is the bidirectional reflectance distribution function at angle of incidence θ, and ω is the beam radius on the mirror. This counter-propagating mode is resonantly built up, so that the fractional power retro-reflected from the OMC from this mirror is:

$$R_{OMC} = BRDF(\theta)\cdot\lambda^2\cdot F^2/\pi^3\omega^2,$$

where *F* is the cavity finesse.

At 4 degree angle-of-incidence, the BRDF of the super-polished mirrors is estimated to be of order 10^{-6} /steridian. The beam radius on the two flat OMC mirrors is 0.5 mm, giving $R_{OMC} = 2.3\times10^{-8}$. As a worst case, we assume that the scattering from each of the 4 OMC mirrors adds coherently, resulting in 16x higher retro-reflected power, or 3.7×10^{-7} (power reflection)[1].

[1] Frolov measured the retro-reflection from the OMC in eLIGO in-situ. Assuming a isolation factor of 10 dB for the AS port Faraday isolator, his measurement corresponds to an OMC reflectivity of 3.6×10^{-8}; see LLO ilog, Jan 28, 2009 and errata.

Displacement noise of this back-scatterer (i.e. motion of the OMC) produces phase noise on the output field, and thus noise in the GW channel. The noise criterion is *(need to verify/document this)*:

$$x_{OMC}\sqrt{R_{OMC}} < 10^{-17}\ \mathrm{m}/\sqrt{\mathrm{Hz}}\,, f > 10\mathrm{Hz}.$$

With the above R_{OMC}, this leads to $x_{OMC} < 10^{-14}\ \mathrm{m}/\sqrt{\mathrm{Hz}}$. With a maximum HAM-ISI motion of $10^{-11}\ \mathrm{m}/\sqrt{\mathrm{Hz}}$, we need a suspension isolation factor of at least 1000 above 10 Hz. The OMC suspension model gives an isolation factor of 2000 at 10 Hz (see LIGO-T0900060).

4.2 Specular reflections

The specular reflections from the 4 diodes (DCPDs and QPDs) are each caught in a V-shaped black-glass beam dump. These dumps are epoxy-bonded to the breadboard.

5 Mechanical design and construction

The OMC is constructed on a fused silica breadboard, with the various components bonded to the breadboard with epoxy. Due to the need to cure and outgas the epoxy at an elevated temperature, any element bonded to the breadboard must also be of fused silica (or similar CTE material) to avoid potentially damaging differential thermal expansion. All of the glass-glass joints are bonded by a UV-cure epoxy, (EMI OPTOCAST 3553-LV-UTF-HM). This epoxy has low viscosity (500 cps, cf. ~2000 cps of EP30-2), and is approved for vacuum. It can make very thin bond layers, estimated to be ~1 micron, which is important for maintaining angles between bonded surfaces. Once the epoxy is applied to a bond, the optical element (prism) can be fine-aligned, then tacked in place by illuminating with UV light. Complete curing of the epoxy is achieved with heat, with the entire breadboard undergoing a 90-100 C bake.

The fused silica breadboard dimensions are: 45 cm long ×15 cm wide ×4.1275 cm thick. The nominal mass is 6.13 kg (not accounting for bevels on edges). The total mass budget for the OMC assembly, for compatibility with the suspension, is 7.0 kg. One side of the breadboard is designated for mounting the OMC optical components. This side is polished with a reasonable flatness specification (flat to 20 micron P-V). This is required because the components are bonded to the breadboard with no adjustment available in their pitch orientations. Therefore, to keep the cavity optic axis well centered on all the components, the breadboard must be reasonably flat; see below for quantitative analysis.

The other side of the breadboard is reserved for: suspension point mounts; balance trim masses; cable routing and connectors. The breadboard is suspended so that the cavity and optical components of the OMC are on the bottom surface, and the suspension points on the top surface.

There are several types of fused silica components bonded to the breadboard. These are listed in the following table, and described below:

Component name	Use	DCC	Vendor
Fused silica breadboard	Mounting of OMC components	D1200105	Sydor Optics
Optical prism	Cavity input/output couplers; beamsplitters; high reflectors	D1101968	Gooch & Housego
Mounting prism	Cavity high reflectors with PZT actuators	D1102069	Mindrum
Diode mount glass block	Photodiode mounting; balance mass mounting; connector bracket mounting	D1102211	Mindrum
Mount bracket	Mount points for suspension wire interface	D1102209	Mindrum
Beam dump	Dumping of specular reflections		

Considering the thermal expansion coefficient of the fused silica breadboard, 0.52ppm/°C for Corning 7980, a 1°C temperature drift of the breadboard will produce a 0.5um change in the round-trip length change of the cavity. Day-to-day variations in the in-chamber temperature are typically smaller than 1°C, but this sets the scale for the minimum cavity length actuation range; see section 6.

The optical layout on the breadboard is shown in Figure 1.

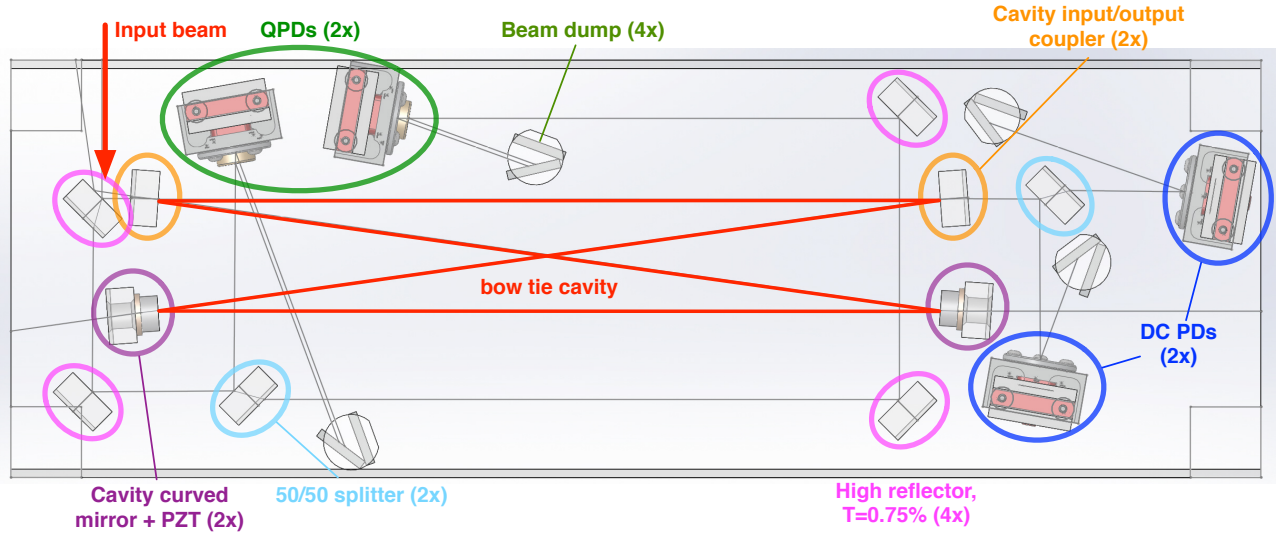

Figure 1. Layout of optical and opto-mechanical components on the OMC breadboard. This layout (without the annotations) is found in D1201439.

5.1 Angle tolerance

The flatness of the breadboard and the perpendicularity of the components bonded to it are specified so as to keep the cavity optic axis well centered on the optical elements (and so parallel to the breadboard mounting surface). We allow a maximum vertical offset of the beam position of 0.5 mm. For a two mirror linear cavity, with a g-parameter of 0.8, the relation between beam offset and mirror angle is roughly: $\Delta x \approx 5L\theta$, where L is the cavity length (0.5 m) and theta the mirror angle (deviation of mirror normal from breadboard plane). For $\Delta x \leq 0.5\,mm$, this gives $\theta \leq 200\,\mu rad = 40\,arcsec$.

The breadboard flatness specification, < 20 microns P-V, over a distance of potentially 20 cm, corresponds to a maximum local angle deviation of about 100 micro-radians.

5.2 Optical & mounting prisms

The dimensions of both of these components were chosen in conjunction with a finite element analysis of the breadboard with prisms mounted. This was done by examining a couple of the resonant modes in the several kHz region, and looking at the deflection of the prism at the position of the cavity beam, for various sizes of prisms. The cavity beam height, relative to the breadboard surface, was chosen independently to be 15 mm; this is as low as possible while still providing adequate space for mounting components such as the photodiodes. The FEA analysis led to the selection of prism dimensions of: 20 mm × 10 mm × 23 mm (W × D × H).

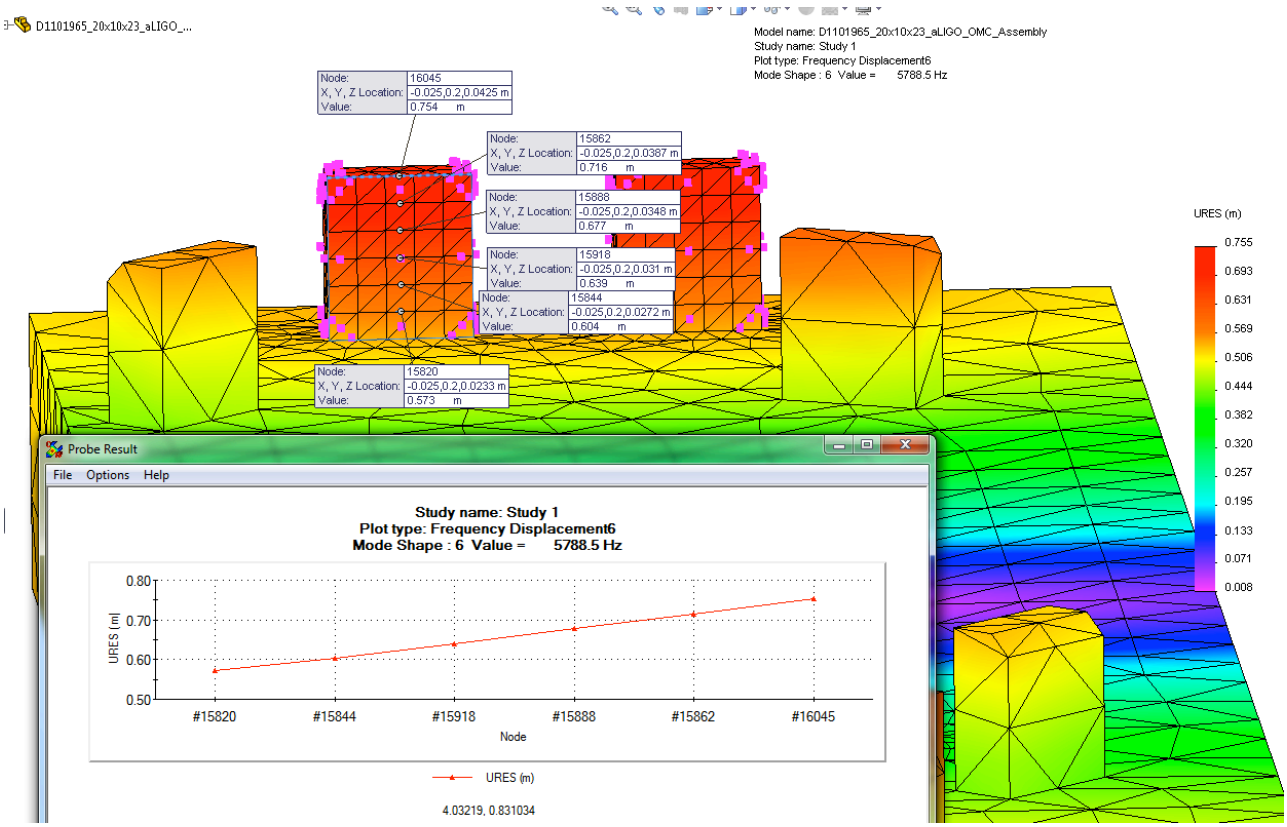

Figure 2. Example of FEA of prism deflection, for a 5.79 kHz mode. The beam spot position is at about the 4th node from the bottom. Prism dimensions are 20mm x 10mm x 23 mm.

To help orient the prisms, each type has a large bevel (1.5 mm wide) on the top rear edge. The mounting prism type has a 9 mm diameter hole through the face, centered on the beam location, for the beam to pass through.

6 Cavity actuators

Each of the two OMC curved mirrors is mounted on a PZT for position (cavity length) actuation. We have used two actuators, rather than just one, to keep the design symmetric and for the utility of having two actuators. The PZT specifications are:

Vendor	Noliac
Model	NAC2124
Size	Ring shape: 15 mm OD, 9 mm ID, 2 mm thick
Stroke	2.8 microns at 200 V
Sensitivity	14 nm/V
Capacitance	470 nF

Each PZT has a large enough stroke to travel several free-spectral-ranges of the cavity. We plan to use both PZTs, splitting their functions as follows: one PZT is used for the length control feedback signal keeping the OMC locked; the other PZT is used to apply the dither modulation used to sense the OMC length, and also as a means of very quickly (< 100 usec) shifting the cavity length by many linewidths to push it off-resonance (i.e., as a fast shutter).

These PZTs have been tested by V Frolov and R DeRosa for their length-to-angle cross-coupling[2]. A typical measured coupling is around 10 μrad/μm, and of about a dozen units tested, the coupling ranges from 6.6—50 μrad/μm. This cross-coupling means that the cavity optic axis will shift as the actuator is displaced. Using a similar argument as above, but with a somewhat tighter tolerance for this 'dynamic' effect, we set a limit that the beam shift over the full stroke of the PZT (2.5 μm) should be no larger than 100 microns. This corresponds to a changing angle of 40 μrad, and therefore a **cross-coupling limit of 16 μrad/μm**. We will therefore select the more uniform PZTs among the batch (of 11 tested so far, 6 fall under this limit and another 2 are very close).

Construction. Each actuated mirror thus consists of three pieces: 0.5" diameter curved mirror; Noliac PZT ring; mounting prism (D1102069). The assembly is shown in the figure below. These three elements are bonded together using MasterBond EP30-2 epoxy.

[2] Documented in the aLIGO wiki: https://awiki.ligo-wa.caltech.edu/aLIGO/PZT_testing

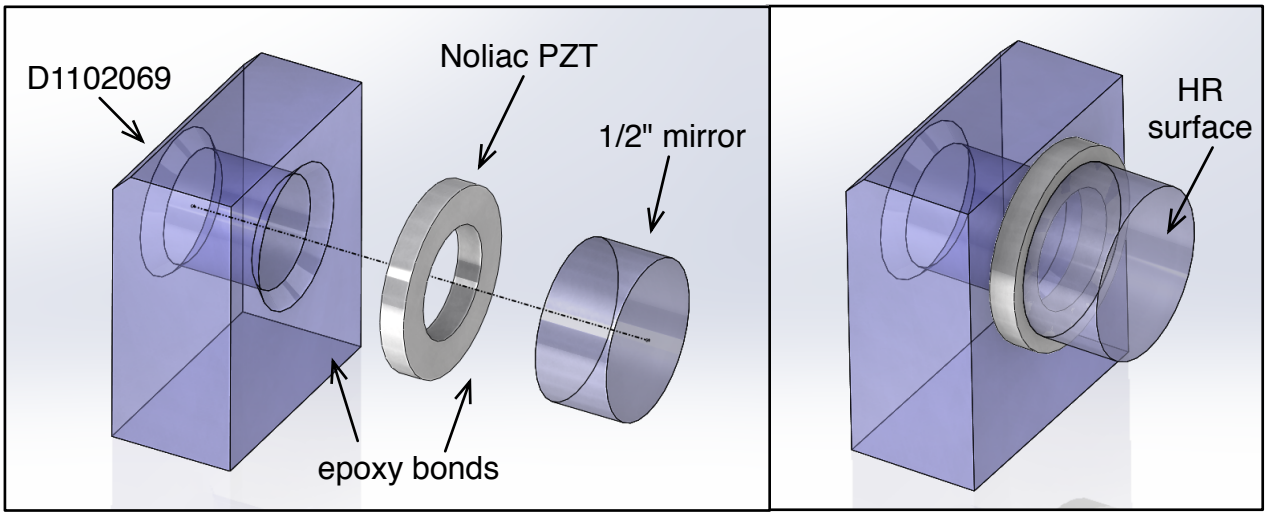

Figure 3. PZT actuated mirror mount (exploded view on left, final assembly on right). The PZT wires (not shown) are soldered to the edge/barrel of the PZT ring (solder composition: Sn96.5/Ag3.0/Cu0.5). The bottom edge of the mounting prism (D1102069) is bonded to the fused silica breadboard.

Shutter function. To protect the DC PDs from the lock-loss pulse, we need to reduce the pulse energy reaching the diodes by a factor of about 500 (50 J stored energy, 100 mJ damage limit); see LIGO-T1000294. In units of free-spectral-range (FSR), the transmission of the OMC is 10^{-3} of the resonant transmission for a cavity length shift of 0.04 away from resonance (essentially, $\sqrt{10^3}/2F$).

The RF sidebands are ± 0.034 (9 MHz) and ± 0.17 (45 MHz) OMC FSR units away from the carrier. The OMC linewidth in these units is 1/400 = 0.025. To stay away from the RF sideband resonances, we can shift the cavity length by anything in the range 0.07—0.1 FSR. Since one FSR is 532 nm of PZT motion, this corresponds to 37—53 nm of PZT motion, which is a voltage step of 2.6—3.8 V. This voltage step should be made in < 100 μsec.

Dither modulation. Dither modulation of the OMC length is used to sense the OMC resonance. The dither is a sine-wave modulation, designed to be applied in the frequency range of 5—20 kHz, and with a maximum amplitude such that peak excursion goes to the 90% transmission point of the resonance curve (normally the dither amplitude will be much smaller than this). This corresponds to a maximum dither amplitude of 0.22 nm, or 16 mV-pk of drive.

7 Photodiodes & mounting

The properties of the photodiodes for the DC readout and the quadrants are shown in the table below. It is important to operate the diodes at a non-zero angle-of-incidence (AOI) so that the specular reflection can be properly dumped. The response versus AOI for 2 mm versions of the C30655 diodes has been measured and is reported in T1100564. With no window, the response of the diode is quite flat up to at least 25 degrees AOI.

	DC PD	QPD
Model	Excelitas C30655	OSI Q3000
Type	InGaAs	InGaAs
Diameter	3 mm	3 mm
Window	removed	yes
Beam diameter	1.04 mm ($1/e^2$)	0.98 mm & 1.2 mm
AOI	10 deg.	10 deg.

Table 2. Properties of the photodiodes used on the OMC.

The mount for the DC PD is shown in Figure 4. Once the cavity has been bonded to the breadboard, the DCPDs are mounted and the precise position of each diode is aligned to the cavity output beam using the adjustment capabilities of the mount. A beam centering tolerance of 0.5 mm is aimed for. The horizontal position of the diode is adjusted by moving the housing within the range of the mounting slots. The vertical position is adjusted using an aluminum shim (various thicknesses available) between the glass mount block and the housing. Once the housings are aligned to the beam, they are not intended to be moved again. A diode can be replaced, without moving the housing, by simply removing the retaining ring and inserting a new diode into the socket. This approach relies on the diode elements being well-centered in their housings. This has been measured for about 20 photodiodes, and the results are reported in T1100639. The diode centers were found to be offset from the center of their housings by on average 80 microns, well within our centering requirement.

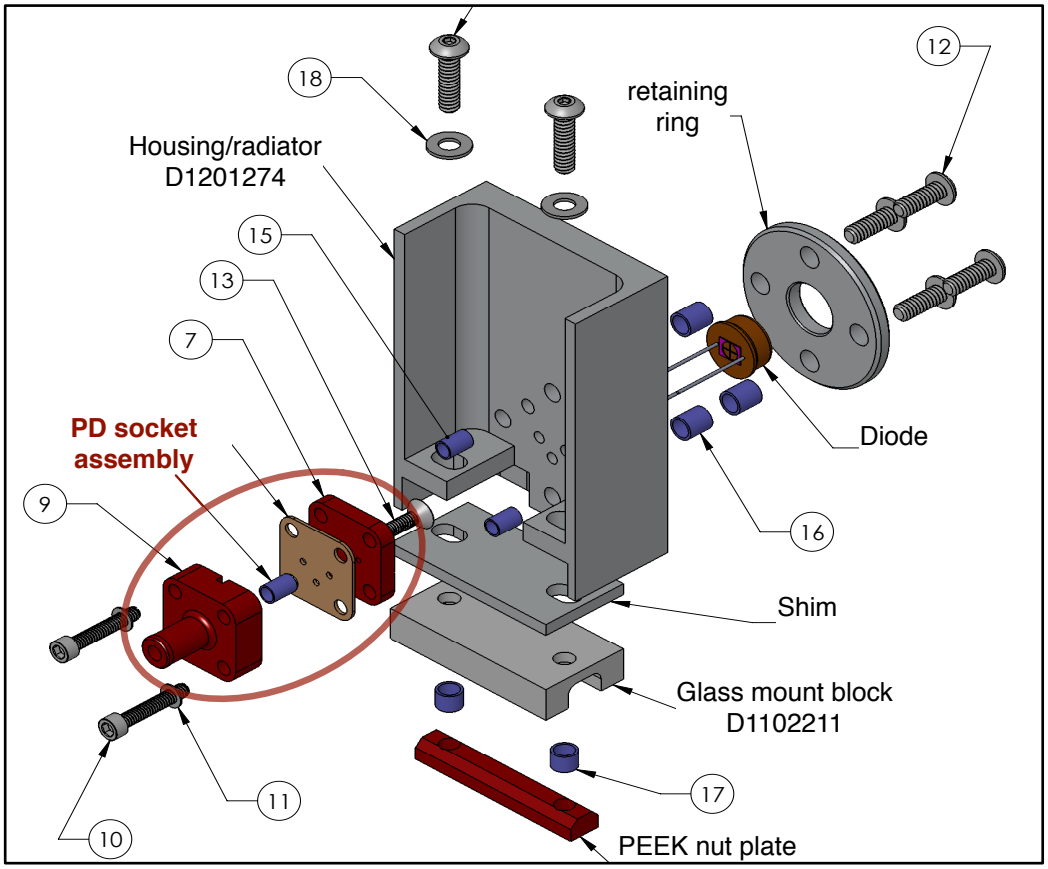

Figure 4. DC photodiode mount assembly: D1201273 (v1). The glass block (fused silica) is bonded to the OMC breadboard. The diode is inserted into the socket assembly (sandwich of PEEK/flex circuit/PEEK) and held in good thermal contact to the housing with the retaining ring. The PEEK nut plate provides compliance for screwing this unit onto the mount block. A set of shims provides vertical position adjustment; slots in the housing provide horizontal adjustment. The faces of the housing are coated with aluminum oxide (plasma spray), to provide a high emissivity for thermal radiation. The blue items are nitronic 60 heli-coils.

The mount assembly for the QPD is similar to that for the DCPD; see D1201279. The main difference is a smaller housing/radiator, and it is not Al_2O_3-coated, since the power dissipated in the QPDs is much smaller.

Power dissipation. The DCPD mounting is designed assuming up to 100 mW of light on each diode, and a reverse bias on the diode of up to 5 V. This corresponds to a power dissipation of up to 0.5 W. At this power level, we aim to limit the temperature rise of the housing to no more than 20C. With an emissivity of 0.9 for the Al_2O_3-coated surfaces, this corresponds to a radiator surface area of about 42 cm^2. The surface area of the housing D1201274 is a bit more than this, though we have not done detailed calculations of the effective radiative area of the shape.

The QPDs will dissipate around 10 mW maximum, so thermal handling is not an issue.

8 Cavity noise

Noise in the length of the OMC cavity can couple into the GW channel either non-linearly (second order power transmission around the resonance peak, or bi-linearly with a rms offset from the peak) or linearly (static offset from the peak). Tests of the OMC coupling in Enhanced LIGO suggests that a safe upper limit for cavity length noise is 3×10^{-16} m/√Hz; see LIGO-G1100903 for the background. This level of length noise would produce a transmitted power noise that is 10x smaller than shot noise for 100 ma of photocurrent, with an offset from resonance of 0.2 pm.

Frolov and DeRosa have made measurements aimed at uncovering the intrinsic noise in the PZTs; see the same wiki entry as referenced earlier. Using a Michelson interferometer, they have established an upper limit to the PZT noise of 6×10^{-16} m/√Hz, close enough to the above limit (which has margin) to be acceptable.

The cavity length noise limit imposes a requirement on the voltage noise of the PZT drivers. This works out to a maximum of 15 nV/√Hz on each PZT (above ~50 Hz).

There will also be thermal noise of the OMC cavity. This hasn't been modeled in any detail, but we can make an order of magnitude estimate using a single degree-of-freedom oscillator model. The on-resonance thermal excitation of such an oscillator, using numbers reasonable for an OMC mode, is:

$$x_{th} = 3\times10^{-15} \cdot \left(\frac{1\ \mathrm{kg}}{m}\right)^{1/2} \cdot \left(\frac{2\ \mathrm{kHz}}{f_0}\right)^{3/2} \cdot \left(\frac{Q}{1000}\right)^{1/2} \mathrm{m}/\sqrt{\mathrm{Hz}}$$

While this is above the limit given in the first paragraph of this section, it is only at the resonant peak. The first eigenmode of the OMC, a bending of the breadboard, is at about 1 kHz; as mentioned above, modes that involve more local motions of the cavity prisms are above a few kHz. More finite-element analysis of the OMC is planned for the future.

9 Photodiode preamps

To be in close proximity to the DC PDs, the preamps for the DC readout are located in the HAM6 vacuum chamber, mounted at the top of the OMC suspension structure. The preamps are the same units used in Enhanced LIGO. The preamp circuits are enclosed in a sealed aluminum box, with hermetic feed-throughs for the electrical connections. The design and performance of these preamps is documented elsewhere (preamp schematic is D060572).

10 Electrical cabling

The design for the electrical cabling from the devices on the breadboard to the top of the suspension structure is shown in Figure 5. At this location, all signals are on 25-pin Dsub connectors, and standard in-vacuum 25pinDsub-to-25pinDsub cables are used to bring the signals out to the chamber feedthroughs.

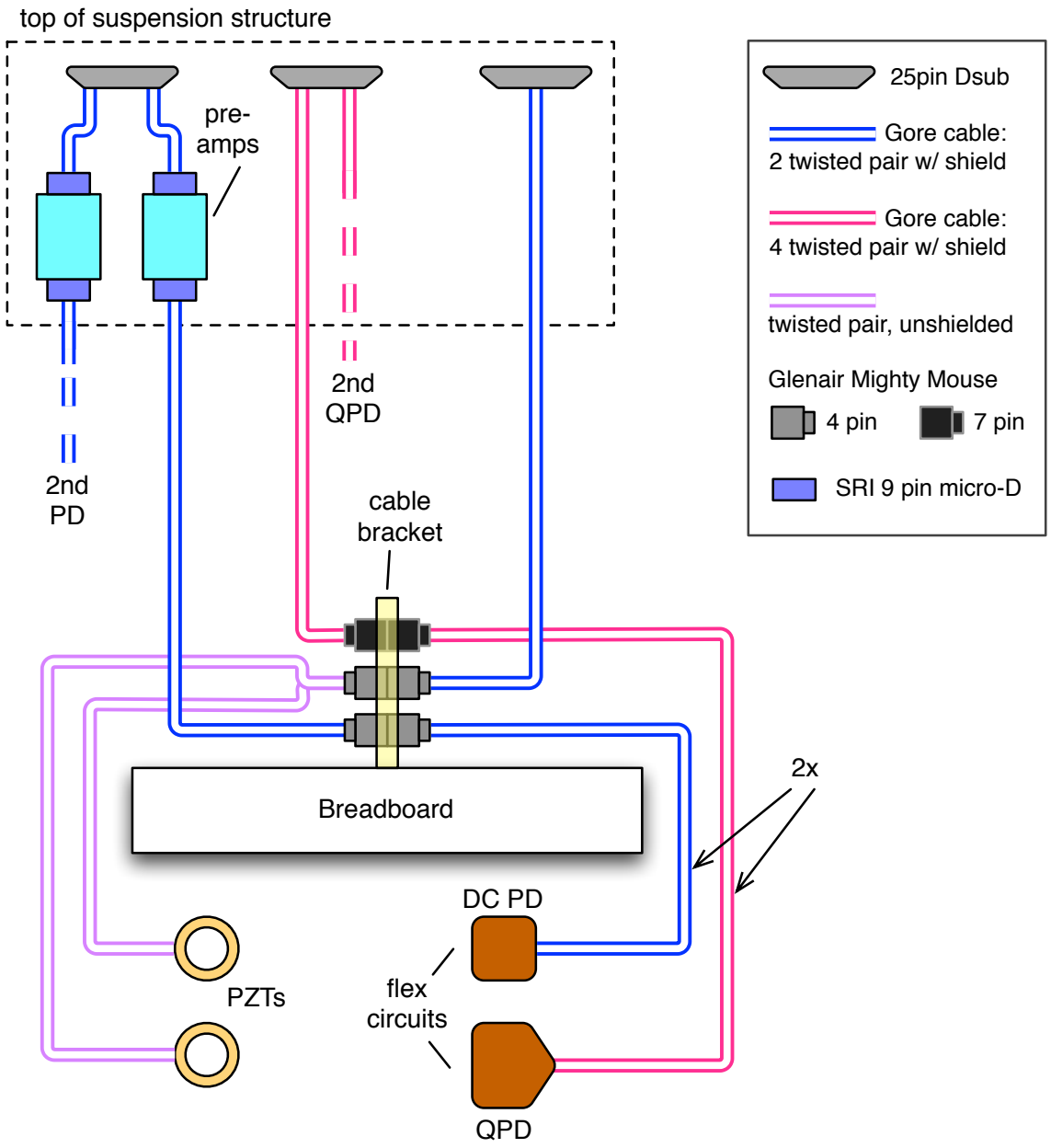

Figure 5. Cabling design for the OMC devices. There are two each of the DCPDs and QPDs; only one of each is shown for simplicity. The Gore cable is a flexible cable, with PTFE insulation, a ePTFE jacket, and 26 awg conductors. The PZT wires are polyimide insulated, 32 awg. The cable bracket (D1300052) mounts to the OMC breadboard by screwing onto two of the glass mount blocks (D1102211). Though not shown, at the breadboard cable bracket and at balance-mass brackets at the top ends of the breadboard, there are cable 'pegs' for routing and strain-relief of the cables as they travel from the bottom to the top of the breadboard. See also **Figure 7**.

11 Suspension interface

The OMC breadboard is suspended from the non-optical side, which is the top side when suspended. There are four suspension points for the four suspension wires. The suspension point interface, shown in Figure 6, is designed to make it easy to install and remove the OMC from the suspension, without having to access the optics side of the breadboard.

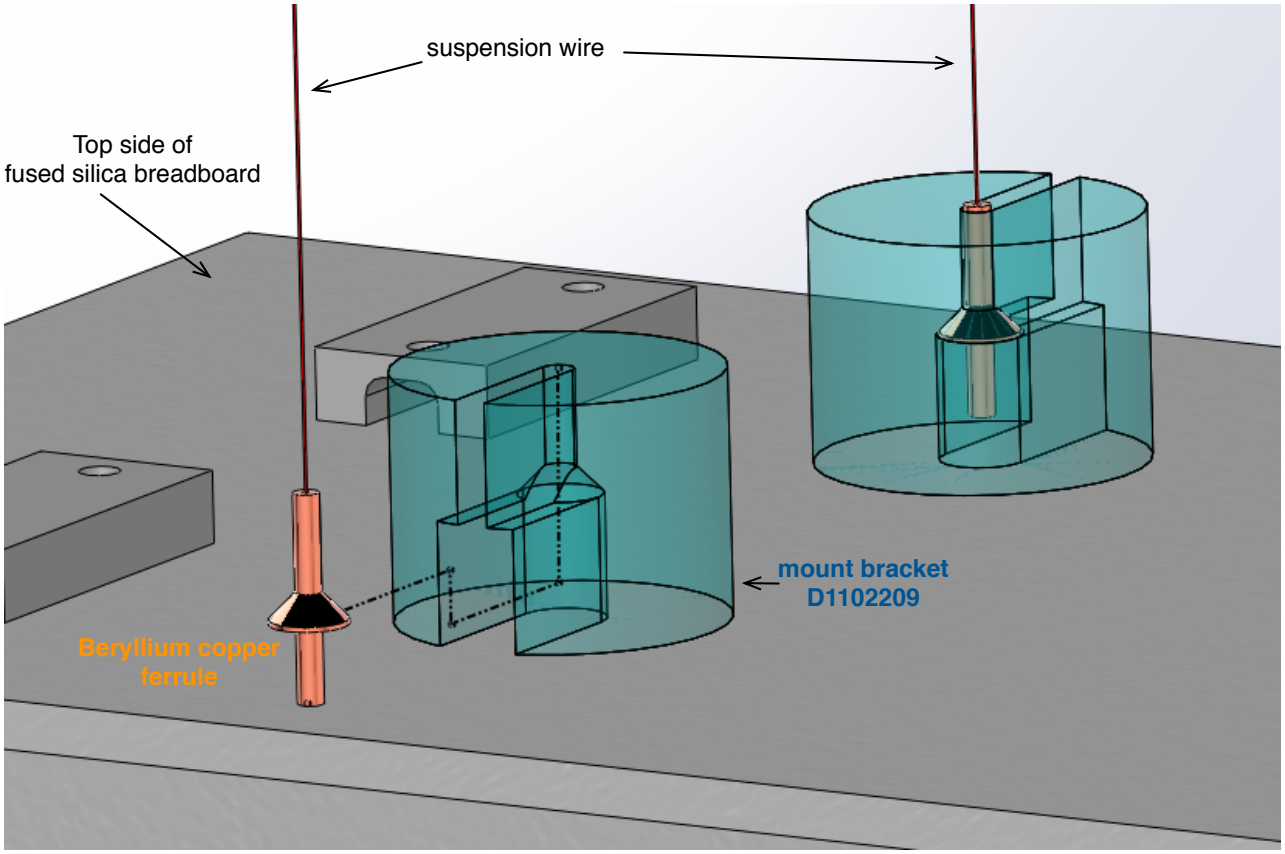

Figure 6. Design for attachment of the suspension wires to the OMC breadboard. A cone-shaped beryllium copper ferrule is affixed to the end of each suspension wire (crimp attachment). This ferrule slips into a slot in the fused silica mount bracket (D1102209), and the conical shape of the ferrule keys into a conical counter-bore in the bracket. There are two such mounting points at each end of the breadboard (other end not shown), four overall. The mount bracket is bonded to the breadboard with UV-cure epoxy. (The u-channel gray blocks in the background are mounts used for balance masses.)

12 Suspension modes

An OMC suspension model from M Barton was used to calculate the eigen-frequencies of the suspension; the following values use a suspension point that is 5 cm above the center-of-gravity of the payload (1 refers to the payload and 2 to the intermediate stage):

Frequency (Hz)	Mode
0.48	yaw2, yaw1
0.70	pitch2, pitch1
0.70	roll2, roll1
1.09	roll2, roll1
1.12	z2, z1
2.12	pitch1, pitch2
2.56	y1, roll1
2.78	pitch1
3.60	yaw1
4.03	pitch1
4.48	z1

13 Balance masses

The total mass of the OMC breadboard, including everything except balance masses, is 6.828 kg. For balance/trim masses, we use the Additional Mass Disks designed for the triple suspension. These come in masses of 100, 50, 20, 10, 5 and 2 grams. They screw onto a bracket, which in turned is mounted to a pair of glass mount blocks; see Figure 7.

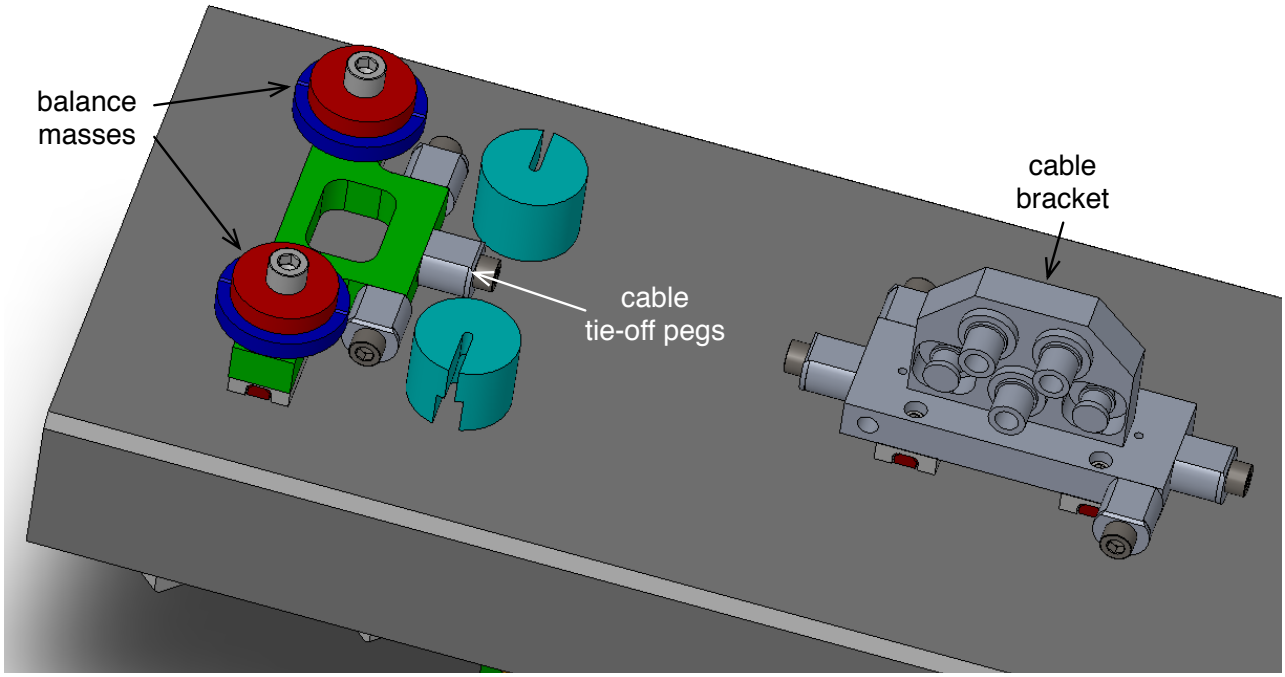

Figure 7. OMC balancing: each end of the breadboard has a bracket (green) onto which balance masses can be added (red and blue disks). The bracket also holds pegs for strain-relieving cables as they are routed from the bottom of the breadboard to the cable bracket; cables are secured to the pegs using aluminum cable wraps. This picture also shows the cable bracket, containing the five cable connections, which is mounted at the center of the top side of the breadboard.

14 Earthquake stops

The design of the earthquake (EQ) stops for the OMC is shown in Figure 8. A key feature is that each EQ stop has only two positions: either ‘in’ for clamping, or retracted/out. The eliminates the need to adjust the gap on each stop when the payload is hung.

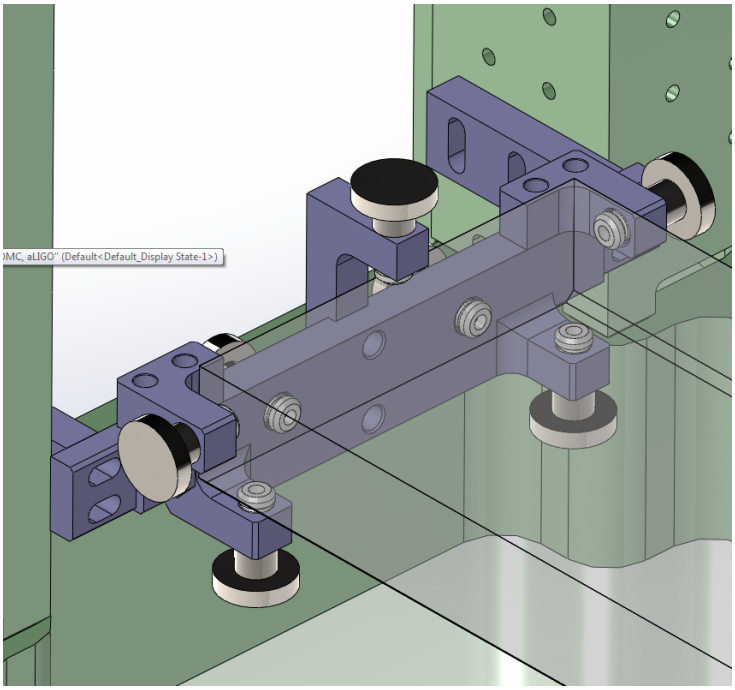

Figure 8. Earthquake stops at one end of the OMC breadboard; the same design exists at the other end of the breadboard. Each end of the board has 6 stops, as shown. The blue brackets attach to the suspension structure, and can be adjusted in position to line up with the breadboard. Each stop is meant to be set in one of two positions—either 'in' or 'out'—by adjustment of the thumbscrew. When 'in' the stop tip contacts the breadboard; when 'out', there is a 1.5 mm gap. The stop tips are made of electrically conductive PEEK.

15 Comparison to Enhanced LIGO OMC

The aLIGO OMC incorporates several changes/improvements compared to the eLIGO design:

- Photodiode mounts redesigned for easier assembly, easier diode replacement, and better visibility of diode
- All mirrors/beamsplitters other than the cavity high-reflectors are a single piece of fused silica (rather than a cylindrical mirror bonded to a rectangular prism); this is not only simpler, but provides better access to optical surfaces for cleaning
- Cavity high-reflectors bonded to PZTs on their back surfaces, providing better access for mirror surface cleaning
- Thermal actuator eliminated; PZT type changed to type with much longer stroke (the thermal actuator had an annoyingly slow response, restricted the clear aperture, and seemed to change the ROC of the mirror with heating)
- Breadboard made of fused silica, rather than ULE (ULE not required, and is more expensive)

- Suspension interface redesigned to be at the top side of the breadboard, for easier hanging and removal; this does increase the position of the wire release point from the CG, raising some of the suspension mode frequencies (most notably the higher frequency mode involving pitch of both stages), but this is not significant to the performance
- DCPD preamps are moved off the breadboard; cable lengths are not much longer than before, and this makes mounting (& servicing) the preamps easier
- More flexible cabling between the OMC and the suspension structure
- Suspension earth-quake stops redesigned for improved usability, and reduced interference with the breadboard